Comparison of experimental and calculated attachment rate constants for $CFCl_3$ and CCl_4 in the temperature range 294–500 K

O. J. Orient and A. Chutjian
Jet Propulsion Laboratory, California Institute of Technology, Pasadena, California 91109

R. W. Crompton and B. Cheung
Atomic and Molecular Physics Laboratories, Research School of Physical Sciences, Australian National University, Canberra, Australian Capital Territory 2601, Australia
(Received 28 November 1988)

Electron-attachment cross sections and rate constants have been measured and calculated for the dissociative attachment processes $e+CFCl_3 \rightarrow Cl^- + CFCl_2$ and $e+CCl_4 \rightarrow Cl^- + CCl_3$. Good agreement over the electron-energy range 1–200 meV is found in energy dependence between present calculated cross sections and experimental (krypton photoionization) cross sections at 300 K. The same calculation, with suitable adjustment of thermal populations, was used to calculate electron-attachment rate constants $k(\bar{\varepsilon})$ in the range 50–600 K. Experimental rate constants for $CFCl_3$ and CCl_4 were measured at temperatures of 294, 404, and 496 K ($CFCl_3$) and 294, 400, and 500 K (CCl_4) using the Cavalleri electron-density sampling method. Good agreement is found between present measurements and calculations, poor agreement with flowing-afterglow Langmuir-probe (FALP) data in $CFCl_3$ at the higher temperatures, and reasonable agreement with FALP data for CCl_4.

I. INTRODUCTION

The electron-attachment properties of a molecular target can be studied in two modes. One may either vary the electron temperature (energy) while holding the target at a fixed molecular temperature, or one may vary both the electron and target temperatures. Different attachment properties are examined in these alternative modes: in the former one studies the attachment cross section or rate constant for a fixed Maxwell-Boltzmann population of the target, while in the latter a varying population mixture of levels is introduced, and the attachment is studied as a function of both electron temperature, and a temperature-varying sum over rotational and vibrational quantum numbers.

A considerable body of data has become available on thermal electron attachment to $CFCl_3$ and CCl_4. Measurements of cross sections[1,2] and rate constants[3–10] have been reported. Also, preliminary theoretical calculations of both quantities have been given for a fixed-temperature target (300 K), and for one having a vibrational-rotational temperature variable in the range 50–600 K.[11] Both theory and experiment[4] gave a negative temperature dependence of the rate constant $k(\bar{\varepsilon})$ for CCl_4 at each mean electron energy $\bar{\varepsilon}$, while for $CFCl_3$ theory predicted a negative temperature dependence, and experiment showed a peak in $k(\bar{\varepsilon})$ at a mean energy $\bar{\varepsilon} \sim 60$ meV (460 K). Intuitively, one would expect both molecules to have somewhat similar behavior, since the underlying attachment cross sections[1,2] showed no significant differences from one another in the electron energy range 1–140 meV.

The flowing-afterglow Langmuir-probe (FALP) technique was used in the first measurements.[4,5] A study was undertaken in the present work to use the Cavalleri electron-density sampling (CEDS) method[3,12,13] to measure $k(\bar{\varepsilon})$ versus $\bar{\varepsilon}$ for both molecules, and over the range of $\bar{\varepsilon}$ (294–500 K) in which the anomaly existed.

Theoretical calculations similar to those carried out in SF_6 (Ref. 14) were applied to $CFCl_3$ and CCl_4. These calculations were based on the theoretical framework of O'Malley for dissociative electron attachment.[15,16] This combination of experiment and theory shows that a negative temperature dependence is exhibited by both molecules, and that the peaking rate constant for $CFCl_3$ observed in the FALP measurements is not reproduced by either our CEDS measurements or theory. In Sec. II we present the experimental and theoretical approaches used. In Sec. III comparisons are given between experiment and theory for both the attachment cross section $\sigma_A(\varepsilon)$ and rate constant $k(\bar{\varepsilon})$ in $CFCl_3$ and CCl_4.

II. EXPERIMENTAL AND THEORETICAL CONSIDERATIONS

A. Experimental determination of $k(\bar{\varepsilon})$

The application of the Cavalleri electron density sampling technique to the measurement of attachment rate constants for thermal electrons has been described previously.[3,12] In summary, the technique is based on the measurement of the rate of loss of thermalized electrons due to diffusion and attachment in a cylindrical glass cell of accurately known geometry (Fig. 1). The initial electron population is produced by a short (~ 5 μs) pulse of x rays from the triode x-ray tube. The gas in the cell is ir-

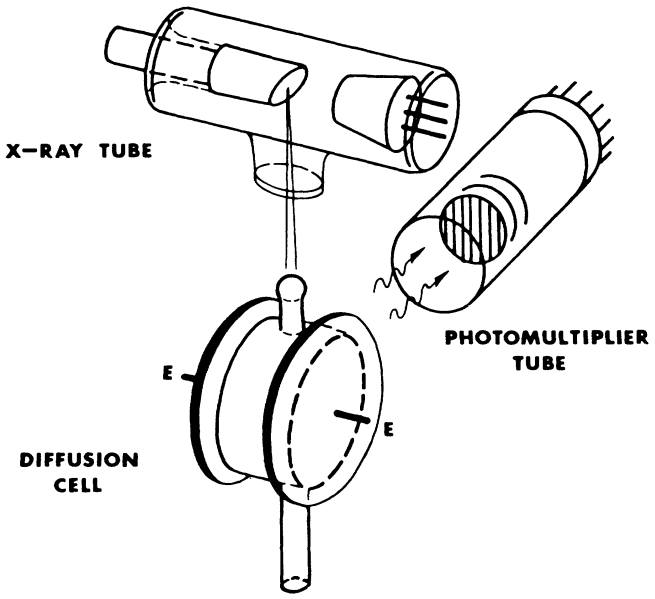

FIG. 1. Schematic diagram of the CEDS experiment for measuring electron-loss rates.

radiated through a beryllium window integral with the x-ray tube and a thin-walled glass bulk on a sidearm of the cell.

The low electron (and ion) densities required to ensure free diffusion necessitate the novel technique devised by Cavalleri[12] for measuring the *relative* population as a function of time. At the sampling time a highly damped rf pulse of large initial amplitude is applied to electrodes external to the cell. The pulse produces local microdischarges at the site of each residual electron. The light output from these discharges is detected by the photomultiplier and provides a relative measure of the decaying electron population at the sampling time. Since the sampling procedure destroys the conditions under which the depletion of the population is being observed, sampling at another delay time requires clearing the cell of all electrons and ions prior to repeating the experiment with a new (hopefully equal) initial electron population.

The cell is housed within a light-tight enclosure which forms the inner wall of an oven for these experiments to determine $k(\bar{\varepsilon})$ as a function of the temperature T. The x-ray tube is mounted on the outside of the enclosure by means of the flange containing the beryllium window.

Data to determine the exponential decay time constant are accumulated by repeating a four-step cycle a large number of times (typically in excess of 10^4). Such a procedure is necessary because of the small number of residual electrons at the time of sampling. The x-ray ionizing pulse initiates each step. In step 1 a sampling pulse follows the x-ray pulse after a delay time t_1. Step 2 is a dummy sequence, without the sampling pulse, for noise sampling and subtraction. In steps 3 and 4 sampling occurs at a larger delay time t_2, chosen such that $t_2 - t_1$ approximates the decay time constant. Alternating the sampling times in this way eliminates errors due to drifts (e.g., in the initial population number and the sampling pulse amplitude). The whole procedure may be repeated using other appropriately chosen pairs of delay times to check that the decay is truly exponential.

The timing sequence and data acquisition are carried out using a dedicated system based on a Z80 microprocessor. The overall linearity of the detection chain, excluding the photomultiplier, was measured and found to be within $\pm 1.5\%$ over the range of amplitudes comprising the recorded pulses.

Nonreproducible results occurred initially at the higher temperatures used in these experiments. These were ultimately traced to spurious signals due to corona discharges external to the cell, and eliminated by flooding the cell enclosure with CO_2. However, nonreproducibility led to a thorough examination of the method of preparing the gas mixtures and to its subsequent behavior in the apparatus itself.

The method of preparing the mixtures, of 1 to 3 ppm of the attaching gas in a nitrogen buffer gas, has been previously described.[3] In stage 1 the mixing chamber, with the valve between the small inner volume and the large volume that surrounds it open, is filled with the attaching gas to the required pressure. The valve is then shut and the large volume evacuated. In stage 2 the large volume is filled with the buffer gas before the tap is again opened and mixing commences.

At partial pressures as low as those of the attaching component in these mixtures, adsorption and desorption could be significant. Desorption from the walls of the large volume of the mixing chamber following stage 1 was shown to be significant if insufficient time were allowed before stage 2 commenced. On the other hand, direct measurement of the pressure of the attaching gas after expansion from the small volume (in the absence of the buffer gas) indicated no significant reduction of the expected pressure ($\sim 5\times 10^{-4}$ Torr) due to adsorption. Additional confidence in the accuracy of the mixture composition came from a comparison of the measured values of $k(\bar{\varepsilon})$ for $CFCl_3$ obtained using the "homemade" gas mixture with those measured using a 2.1-ppm mixture from a commercial supplier (CIG, Spectraseal α-grade standard). The results agreed to within 2.5%, the uncertainty of the composition of the commercial gas mixture being conservatively estimated as $\pm 5\%$.

While there was considerable confidence in the composition of the initial mixture, care was taken to eliminate, or allow for, subsequent changes in composition. First, it was found to be necessary to passivate the walls of the diffusion cell and associated glass ballast volume before admitting the sample of gas in which the measurements were to be made. Second, in the case of CCl_4, but not $CFCl_3$, there were two sources of time dependence which had to be allowed for. The first of these was a small time dependence due to a loss of CCl_4 in the supply reservoir. The second, somewhat larger, dependence resulted from loss of CCl_4 within the diffusion cell and ballast reservoir when the temperature was raised to 500 K. Both effects will be discussed in Sec. III A.

When the electron population is sampled at time $t > \tau_{D_1}$ the diffusion time constant for the fundamental diffusion mode, the time dependence of the electron population N_e is given by

$$N_e(t) = N_e(0) e^{-t/\tau} ,$$

where

$$\tau^{-1} = \tau_{D_1}^{-1} + \nu_{\text{at}} ,$$

and ν_{at} is the attachment collision frequency.

In these experiments, however, it is not possible to satisfy this condition even using mixtures containing only ~ 1 ppm of the attaching gas; that is, the most dilute mixtures that could be made with the required accuracy and used subsequently with reasonable confidence that effects such as those described above would not significantly affect the results. It was therefore necessary to use the procedure described by Petrović and Crompton[12] based on the use of an *effective* diffusion coefficient D_{eff} determined from measurements in the pure buffer gas at the same pressure and at the same sampling times as those used for measurements in the mixture. Since, for most of the measurements, attachment was by far the larger loss mechanism (i.e., $\nu_{\text{at}} \gg D_{\text{eff}}^{-1}$) D_{eff} did not have to be determined with high accuracy.

For each gas, measurements were made at 294 K and temperatures close to 400 and 500 K using mixtures containing 1.20 and 2.40 ppm of the attaching gas in N_2. Most of the measurements were made at a total pressure of 3.0 kPa, with only a few measurements at another pressure (2.0 kPa) since any dependence of the results on total gas pressure had been extensively investigated earlier by Crompton and Haddad[3] and shown to be negligible.

B. Theoretical approach

1. Defining equations

As in an earlier study of SF_6,[14] electron attachment cross sections $\sigma_A(\varepsilon)$ were calculated in the range 1–200 meV in an approximation to O'Malley's theory of dissociative attachment.[15,16] A diatomiclike harmonic-oscillator model of the $CFCl_3$ and CCl_4 electronic ground states was adopted which included the known dissociation energies D_e, equilibrium distances R_0, vibration frequencies of each normal mode ω_i, and rotational constants B_v. These quantities were used to calculate the attachment cross section from each vibration-rotation level, as well as the population of that level from the partition function. A rotational barrier of the form $B_v J(J+1)/R^2$ was also included, where R is the $CFCl_2$-Cl or CCl_3-Cl internuclear separation. For the negative-ion ground state, the final potential energy curve $V_f(R)$ was expanded about the neutral-molecule equilibrium distance R_0 in the form

$$V_f(R) = -V_0 - V'\Delta R + \tfrac{1}{2}V''\Delta R^2 , \quad (1)$$

where $\Delta R = R - R_0$, and where the constants V_0, V' and V'' were obtained from a fit to the experimental $\sigma_A(\varepsilon)$ at 300 K for each molecule.

The basic approach follows closely that of Ref. 14. We present below a summary of the calculational method, with more emphasis on differences from the earlier calculation. We write the attachment cross section $\sigma_A^{v\omega,J}(\varepsilon)$ for the vth harmonic of the ωth normal mode and rotational level J, as

$$\sigma_A^{v\omega,J}(\varepsilon) = (4\pi^2 g/k^2)(\Gamma_a/\Gamma_d)|\bar{\chi}_{v\omega,J}(R_\varepsilon - i\Gamma_a/\Gamma_d)|^2 \times \exp[-\rho(\varepsilon)] , \quad (2)$$

where k is the electron momentum, Γ_a and Γ_d are the autoionization and dissociation widths, respectively, g is a spin degeneracy factor (taken as 2), and R_ε is the turning point in the final state at energy ε. The quantity $\bar{\chi}_{v\omega,J}$ is the complex overlap integral between the $v\omega$th level, and the continuum of $CFCl_3^-$ or CCl_4^- levels degenerate with it. These continuum levels are described by a modified δ function which includes the finite change in nuclear momentum during attachment. The $\bar{\chi}_{v\omega,J}$ are calculated for each level $v\omega,J$ as described in Refs. 14 or 15. Finally, $\rho(\varepsilon)$ is twice the imaginary part of the complex final-state phase shift, and $\exp[-\rho(\varepsilon)]$ is the survival probability[17] with $\rho(\varepsilon)$ given by

$$\rho(\varepsilon) = \int_{R_\varepsilon}^{R_c} \frac{\Gamma_a(\varepsilon(R))}{\hbar v(R)} dR . \quad (3)$$

Here $v(R)$ is the classical velocity of the outgoing particles, and R_c the crossing point between the neutral-molecule and negative-ion states. In practice, due to the small range of the integral in Eq. (3) and the small width Γ_a, values of $\rho(\varepsilon)$ in the present work were again found to be less than 10^{-3}, so that $\exp[-\rho(\varepsilon)]$ could be taken as unity for all $v\omega,J$. Furthermore, since *ab initio* calculation of the autoionization width $\Gamma_a(\varepsilon)$ is extremely difficult, we chose to parametrize it as a function of ε in the form $\Gamma_a(\varepsilon) = \Gamma_a^0 \varepsilon^{l+1/2}$, where l is the angular momentum component of the captured electron. Γ_a^0 is a constant obtained from an overall normalization of the cross section by integrating $\sigma_A(\varepsilon)$ with a Maxwellian electron energy distribution function to yield the CEDS-measured rate constant. The above form of parametrization is not arbitrary, but gives the correct Wigner threshold law[18] of $\sigma_A(\varepsilon) \sim \varepsilon^{-1}\Gamma_a(\varepsilon) \sim \varepsilon^{l-1/2}$. In the present case, $l=0$ and one has the limit (usually achieved for $\varepsilon < 10$ meV) $\sigma_A(\varepsilon) \sim \varepsilon^{-1/2}$.

2. Molecular symmetries and thermal populations

As was the case for SF_6 the initial and final electronic states in the attachment process are of the totally symmetric A_{1g} representation. Moreover, one has a strong enhancement at the target of the s-wave component of the incoming electron, and hence the perturbing electric field will be spherically symmetric. We thus take the initial distortion of the nuclear frame to correspond to a movement in the symmetric stretch coordinate (the a_1 breathing mode for T_d and C_{3v} symmetries). Thus, as an approximation to the multidimensional nature of the neutral-molecule–negative-ion crossing, one describes

the surface, in the Franck-Condon region, by a single coordinate R.

Thermally populated levels $v\omega$ in Eq. (2) were taken to be of the a_1 type. For example, in $CFCl_3$ (point group C_{3v}) an excitation of the type $\omega_4(e)+\omega_6(e)$ would be included, since the direct product $e\otimes e=a_1+a_2+e$ contains a_1, whereas ω_4 alone would not be included since it transforms as e. In CCl_4 (point group T_d) an excitation of the type $3\omega_2$ would be included. A total of ten such levels for $CFCl_3$ and nine for CCl_4 were included in the calculation of thermal populations and cross sections (see next subsection). In addition, as a test a second set of levels were included in which CCl_4 was assigned C_{3v} symmetry arising from a single ^{37}Cl atomic substitution for one of the more abundant ^{35}Cl atoms. The resulting C_{3v} calculations led to eight significantly populated levels. There was less than a 5% difference in the final $\sigma_A(\varepsilon)$, and the C_{3v} and T_d cross sections were averaged together.

From known energies of the vibrational modes in $CFCl_3$ (Ref. 19) and CCl_4 (Ref. 20), and known rotational constants,[21,22] the thermal population $b_{v\omega,J}$ of each of the a_1 levels was calculated from standard Boltzmann expressions for a particular state S of the system. Each state consisted of the set of excitations of the a_1 normal modes ω_i, each excited v times. Because of the high J's involved, a histogram sampling of the rotational distribution was taken (see Fig. 1 of Ref. 23), similar to that carried out for SF_6. The cross section of each state $\sigma_A^S(\varepsilon)$ is then written as

$$\sigma_A^S(\varepsilon)=\sum_{v\omega}\sum_J b_{v\omega,J}\sigma_A^{v\omega,J}(\varepsilon)\ , \tag{4}$$

and the final cross section

$$\sigma_A(\varepsilon)=\sum_S \sigma_A^S(\varepsilon)\ . \tag{5}$$

Ten states S were taken for $CFCl_3$ and nine for CCl_4 (eight for the C_{3v} case). The calculated $\sigma_A(\varepsilon)$ was found to be insensitive at the 2% level to additional levels, so that the sum had "converged" in S for each molecule. The largest contribution to $\sigma_A(\varepsilon)$ came from the ground state ($v=0$ for all ω_i) because of its greatest fractional population $b_{v\omega,J}$.

Finally, the attachment rate constant $k(\bar{\varepsilon})$ was calculated at each $\bar{\varepsilon}$ (or T) from the expression

$$k(\bar{\varepsilon})=(2/m)^{1/2}\int_0^\infty \sigma_A(\varepsilon)\varepsilon^{1/2}f(\varepsilon)d\varepsilon\ , \tag{6}$$

where $f(\varepsilon)$ is the Maxwellian electron energy distribution function at mean energy $\bar{\varepsilon}$. The error in digitizing and numerically integrating the $\sigma_A(\varepsilon)$ curves at each T was held to less than 1%. The overall normalization constant for the attachment cross section was given by the present experimental values of $k(\bar{\varepsilon})$ at 300 K, taken as 2.38×10^{-7} cm^3/s for $CFCl_3$, and 3.79×10^{-7} cm^3/s for CCl_4.

III. RESULTS AND DISCUSSION

A. Experimental values of $k(\bar{\varepsilon})$

1. $CFCl_3$

Important differences were noted between this set of measurements and the measurements made in CCl_4 [see (2.) below].

(i) There was no significant difference in results taken with samples of gas drawn from the supply reservoir at different times; that is, no significant dependence of results on the age of the gas mixture.

(ii) At 500 K there was no significant time dependence in the results.

The absence of time dependence meant that there was much higher repeatability in the measured time constants for $CFCl_3$ than for CCl_4. For example, at 500 K where the results for CCl_4 were subject to both sources of variability, the rms deviation of results of 15 determinations of τ carried out over 3 days was 0.7%. Fresh samples of gas were used for each of the three sets of five determinations comprising the total.

The results presented in Table I were taken with a mixture containing 2.40 ppm of $CFCl_3$ in N_2 at a pressure of 3 kPa, a choice of gas mixture and pressure that optimized the accuracy of the measurements. Since the results at room temperature agreed to within 0.5% with the result obtained by Haddad and Crompton[3] from measurements using two mixture compositions (3.23 and 6.46 ppm) and pressures in the range 1.0–2.5 kPa, it was not considered necessary to vary these parameters extensively. However, one set of measurements, at 294 and 500 K, was made with a 1.20-ppm mixture. At each temperature the result in this mixture was 7% to 8% lower, that is, the temperature dependence was the same but the absolute values significantly lower. It was subsequently found that the ultrahigh vacuum (UHV) valve isolating the two sections of the mixing chamber had failed to close completely between stages 1 and 2 of the mixture preparation, leading to some loss of $CFCl_3$ and, hence, a lower partial pressure in the mixture than calculated.

The overall uncertainty of the values of $k(\bar{\varepsilon})$ is estimated to be less than 5%, the largest contributor being an uncertainty of 2% to 3% in the mixture composition. The other contributors are: statistical uncertainty, 0.5%; gas number density, 1%; linearity of detection system, 1%; $\tau_{D_{\text{eff}}}$, 0.5%. Thus the *relative* uncertainty of the results recorded at the different temperatures is estimated to be less than 3%.

TABLE I. Measured values of the attachment coefficient $k(\bar{\varepsilon})$ for $CFCl_3$.

T (K)	$k(\bar{\varepsilon})$ (10^{-7} cm^3/s)
294	2.38
404	2.16
496	2.01

2. CCl_4

The larger value of $k(\bar{\varepsilon})$ in CCl_4 meant that it was preferable to use a mixture with a smaller mole fraction of the attaching gas. Therefore, the most extensive set of measurements was made with a 1.20-ppm mixture at 3.0 kPa, with some additional measurements using a 2.40-ppm mixture, also at 3.0 kPa.

Two sources of time dependence of the measured time constant were observed. Measurements made at 294 K with the 1.20-ppm mixture showed a progressive increase of about 7% over a period of 9 days. Since each of the measurements was made with a fresh sample of gas from the mixing chamber (constructed from type 316 stainless steel and having a volume of 5 liters; initial pressure ~65 kPa) it was concluded that this increase was due to a slow depletion of CCl_4 in the mixture. Therefore, corrections were made to these results, and to those at 400 and 500 K, depending on the age of the samples at the time of measurement. The agreement between the results after correction supported the validity of this procedure.

A second source of time dependence was loss of CCl_4 in the Cavalleri cell and associated ballast volume at 500 K; there was no observable loss at 294 and 400 K. The loss rate of approximately 2%/h always occurred and was independent of whether or not the experiment was running; that is, the loss was not attributable to the effect of the initial x-ray ionization or to the sampling pulses. Each result at this temperature was therefore obtained by extrapolating a set of five measurements, taken over a total period of about 10 h, to zero time. A typical set is shown in Fig. 2.

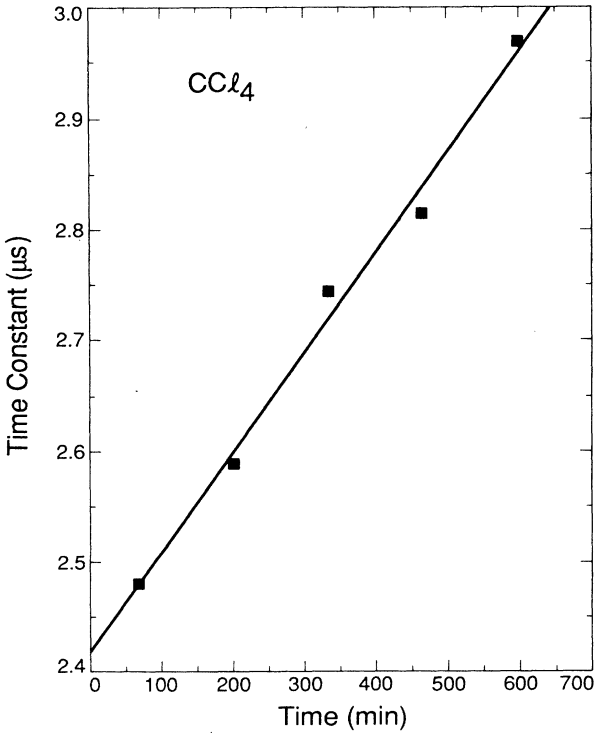

FIG. 2. A sample of the results showing the time dependence of the measured time constant due to loss of CCl_4 in the glass CEDS cell and ballast volume at 500 K. Gas pressure, 3.0 kPa; mixture concentration, 2.40 ppm.

The final results for the two-mixture concentrations are shown in Table II, together with some of the data (in brackets) before correction for the age of the sample. Only those uncorrected results are shown that were either recorded on a single day, or are the averages of results recorded on successive days. The mixtures varied in age from 3 or 4 days at the time of measurement to 10 or 11 days (e.g., the results for the 2.40-ppm mixture at 400 K). Results at 294 K for the 1.20-ppm mixture (eight sets in all) were obtained over a period of nine days and are not shown since they required varying corrections depending on the age of the sample.

The uncertainty associated with the results for CCl_4 is somewhat larger than that for the $CFCl_3$ results due to the variability in the mixture composition, notwithstanding the good agreement between the corrected results at 400 and 500 K. We have somewhat arbitrarily assigned an additional ±3% uncertainty on this account. Nevertheless, we believe an overall uncertainty of ±8% in the final results may be conservative, and we would expect the *relative* uncertainty in the results at the three temperatures to be less than 5%. Finally, we believe it unlikely that, for either gas, our results are significantly affected by secondary dissociative attachment to unstable molecular radical species formed in the initial dissociative attachment process, as discussed in the recent paper by Adams *et al.*[5] These authors have shown that secondary attachment becomes significant when the initial electron density $n_e(0)$ is of the same order as the density n_r of the attaching species. In our experiments we estimate this ratio to be of the order of 10^{-8} or less.

B. Results of calculations

Calculations were carried out by variation of the parameters V_0, V', and V'' [see Eq. (1)] and normalization to the present CEDS-measured $k(\bar{\varepsilon})$ at 300 K. The small difference between the temperature of the calculations and the CEDS data (294 K) was accounted for by interpolation of the latter. We show in Figs. 3 and 4 results of calculated $\sigma_A(\varepsilon)$ at 300 K for $CFCl_3$ and CCl_4, respec-

TABLE II. Measured values of the attachment coefficient $k(\bar{\varepsilon})$ for CCl_4 after corrections for time dependences. Values in square brackets are data before correction for the age of the sample.

Conc. of CCl_4 in N_2 (ppm)	$k(\bar{\varepsilon})$ (10^{-7} cm^3/s)		
	$T=294$ K	$T=400$ K	$T=500$ K
1.20	3.75	2.94	2.33
		[2.86(5)]	[2.23(5)]
2.40	3.83	2.97	2.32
	[3.72]	[2.75(5)]	[2.19]
Average value	3.79	2.96	2.33

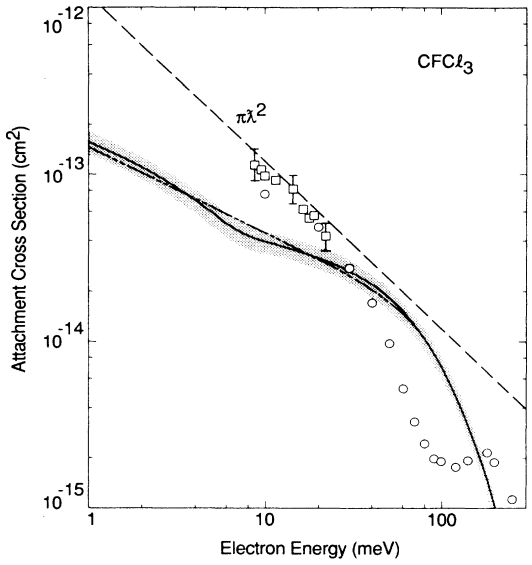

FIG. 3. Electron-attachment cross sections at 300 K for $CFCl_3$. Experimental data are from drift-tube unfolded rate constants (○), high-Rydberg-level collisional ionization rate constants (□), and the krypton photoionization technique (——, with errors indicated by shading). Present calculation is indicated by the dashed curve (——--——) which becomes identical to the photoionization curve at $\varepsilon > 80$ meV. The maximum s-wave attachment cross section $\pi\lambda\!\!\!^{-2}$ is shown (— — —).

tively. Also shown are experimental cross sections from high-Rydberg-level collisional ionization experiments,[8–10] from unfolding rate constant data in swarm experiments,[6,7] and from the krypton photoionization

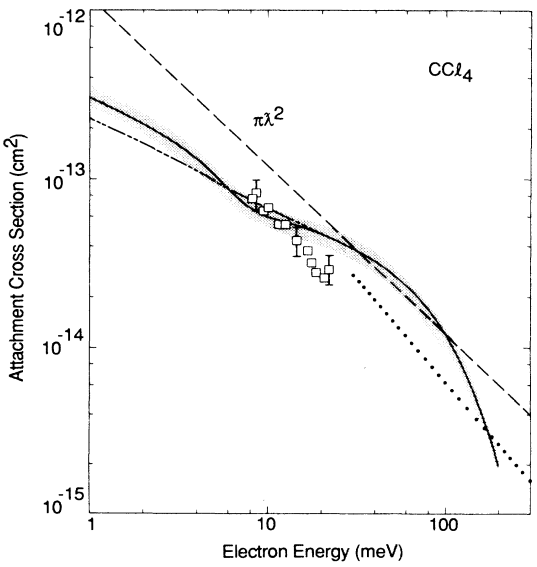

FIG. 4. Electron attachment cross sections at 300 K for CCl_4. Legend is the same as for Fig. 3, except drift tube-unfolded cross sections (· · ·) are from Ref. 7.

method.[1,2] Agreement among the various experimental data is reasonable, and was discussed earlier.[1,2] We only point out that both the swarm cross section and the normalization of the photoionization cross section shown in Fig. 4 of Ref. 2 were based on earlier swarm data[7] that led to a value of $k(\bar{\varepsilon})$ of 2.95×10^{-7} cm^3/s. The present CEDS result of $k(\bar{\varepsilon})=3.79\times10^{-7}$ cm^3/s is higher by a factor of $3.79/2.95=1.28$, and hence the cross sections in Fig. 4 should be multiplied by 1.28. Other evidence[2,4,5] supports the larger cross sections and rate coefficients.

One finds good agreement between present calculations and photoionization results for both $CFCl_3$ and CCl_4 in the range $1\le\varepsilon\le200$ meV. The photoionization results and theory for CCl_4 extend slightly above the s-wave limit in the range 30–90 meV, the experimental excursion being within the error limits. As an experimental check, the slope γ of the cross section in this range was measured again using a new cylindrical ion extraction grid structure.[24] The measured value was $\gamma=5.49\times10^{-2}$ eV, which compares favorably with the value[2] of 5.61×10^{-2} eV. Another likely explanation could be that there is some p-wave contribution to $\sigma_A(\varepsilon)$ at these higher energies. The behavior of this $l=1$ cross section was shown in SF_6 [see Fig. 1 of Ref. 14], and can have maximum value of $(2l+1)\pi\lambda\!\!\!^{-2}=3\pi\lambda\!\!\!^{-2}$ rather than $\pi\lambda\!\!\!^{-2}$.

The neutral and final (negative-ion) potentials obtained for $CFCl_3$ were[25]

$$V_i(R)=-6.10(1.760/R)^6+3.05(1.760/R)^{12}+7.95\times10^{-5}J(J+1)/R^2\ ,$$

$$V_f(R)=-3.042-2.30(R-1.760)+8.0(R-1.760)^2+7.95\times10^{-5}J(J+1)/R^2\ ,$$

and for CCl_4 (T_d symmetry)

$$V_i(R)=-6.16(1.766/R)^6+3.08(1.766/R)^{12}+7.75\times10^{-5}J(J+1)/R^2\ ,$$

$$V_f(R)=-3.072-2.00(R-1.766)+11.0(R-1.766)^2+7.75\times10^{-5}J(J+1)/R^2\ .$$

For the case of one ^{37}Cl substitution (C_{3v} symmetry) the coefficient of the $J(J+1)/R^2$ term was 7.61×10^{-5}. The crossing points between the initial and final states were 1.7635 Å and 1.7700 Å for $CFCl_3$ and CCl_4, respectively. The values of Γ_a^0 were 6.55×10^{-6} eV ($CFCl_3$), 1.031×10^{-5} eV (CCl_4, T_d), and 1.874×10^{-5} eV (CCl_4, C_{3v}). The values of $\sigma_A(\varepsilon)$ and $k(\bar{\varepsilon})$ reported here were taken as an average, over the isotopic abundances, of the values calculated in each symmetry.

The same parameters V_0, V', V'', and Γ_a^0 calculated at 300 K were used for calculations in the range 50–600 K. The only adjustments made were in values of $b_{v\omega,J}$ calculated from the different Boltzmann populations at each T. The sum $\sigma_A^S(\varepsilon)$ was then calculated at each ε, and hence $\sigma_A(\varepsilon)$ and $k(\bar{\varepsilon})$ from Eqs. (5) and (6), respectively. We show in Figs. 5 and 6 the calculated variation of $k(\bar{\varepsilon})$ with $\bar{\varepsilon}$ or T. We show also the CEDS results of the

present work, and previous swarm[6,7] and FALP (Refs. 4 and 5) data. Not shown in Fig. 5 is the rate-constant value of Crompton and Haddad at 295 K which lay within the present error bars at 294 K.

It is clear from Fig. 5 that both the present CEDS results and theory give a negative temperature dependence in $CFCl_3$. In fact, if one were to ignore the changes in v,J populations, changes in electron temperature alone would yield $k(\bar{\varepsilon})$ *versus* $\bar{\varepsilon}$ curves between 300 and 600 K that would be falling at a rate 0.93 (0.80 for CCl_4) the rate of the fully calculated curves. For the most part, the Maxwellian distribution is "sliding up and down" the $\sigma_A(\varepsilon)$ curve (Fig. 3) as a function of $\bar{\varepsilon}$. Since only the Cl^- production channel is open in the range $0 \leq \varepsilon \leq 200$ meV considered here, one would not expect any flattening, or peaking, in the $k(\bar{\varepsilon})$ curve. Such a flattening, for example, was observed in SF_6 (Ref. 14) to arise from an additional channel to produce SF_5^- at higher $\bar{\varepsilon}$. The FALP results show an incorrect trend in the $CFCl_3$ rate constant towards higher $\bar{\varepsilon}$. No explanation can be given at the moment for this variation, except that a similar anomalous peak was observed for SF_6.[4,14]

Similarly, one would intuitively expect that a negative temperature dependence should be found for CCl_4. Production of Cl^- is the only channel open in the range $0 \leq \varepsilon \leq 200$ meV, and the behavior of $\sigma_A(\varepsilon)$ with ε (Fig. 4) is similar to that for $CFCl_3$. Both present experiments

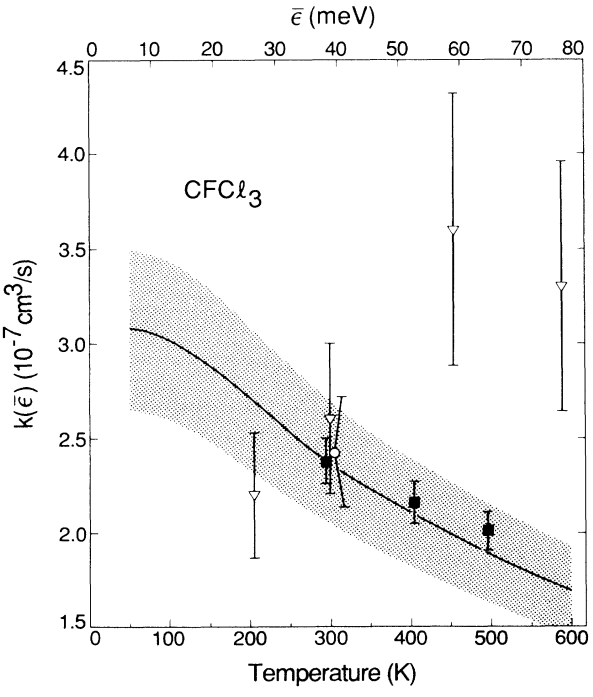

FIG. 5. Electron attachment rate constants as a function of mean electron energy for $CFCl_3$. Experimental results are from FALP measurements of Smith *et al.* (Ref. 4) (▽), drift tube results of McCorkle *et al.* (Ref. 6) (○), and present CEDS results (■). Present calculations are given as solid line (——) with errors indicated by shading.

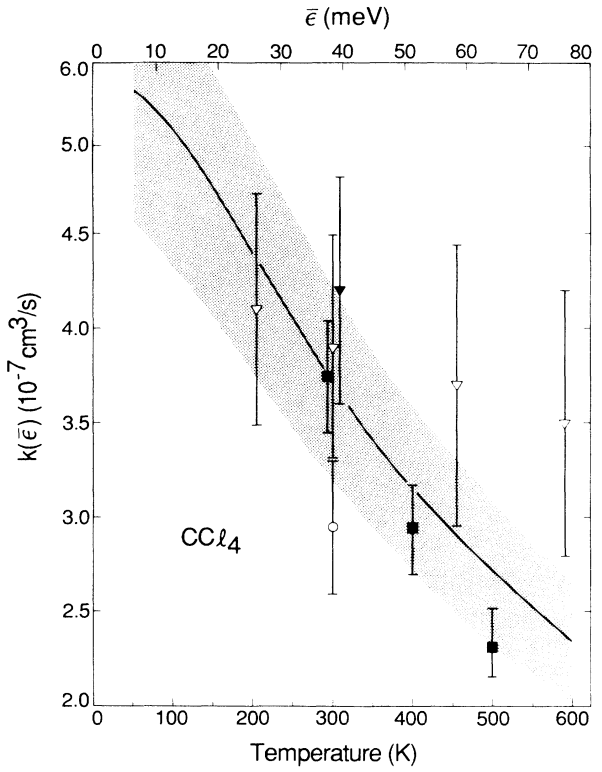

FIG. 6. Electron attachment rate constants as a function of mean electron energy for CCl_4. Legend is the same as in Fig. 5, except that drift-tube result (○) is from Ref. 7, and additional FALP measurement (▼) at 300 K from Ref. 5.

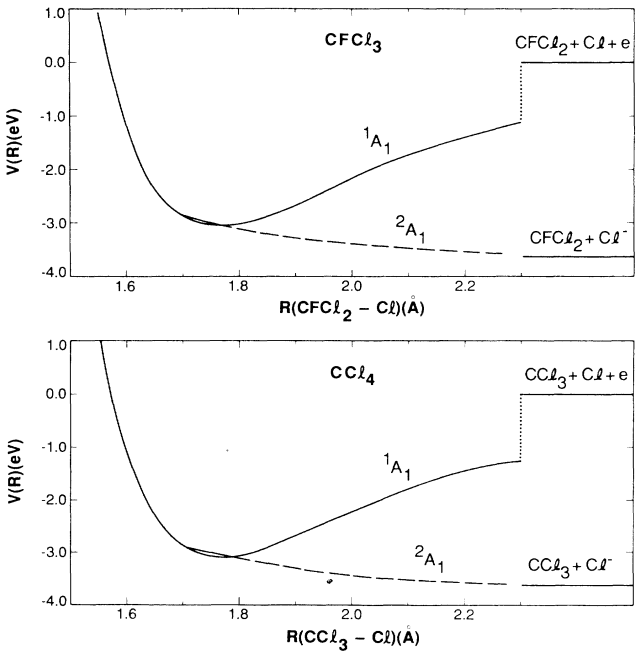

FIG. 7. Approximate, diatomiclike potential energy curves for $CFCl_3$ (top) and CCl_4 (bottom). The relevant negative-ion curve is indicated as the solid line in the Franck-Condon region, and dashed line towards the dissociative attachment asymptote.

and theory (Fig. 6) bear this out: the rate constant $k(\bar{\varepsilon})$ is monotonically decreasing with increasing $\bar{\varepsilon}$. This trend is also present in the FALP results. Approximate, one-dimensional potential-energy curves for $CFCl_3$ and CCl_4 are shown in Fig. 7. These curves are based on the known data for the neutral target,[25] and data for the negative ion calculated here.

Agreement in $CFCl_3$ between the slope of the present calculations and CEDS data (Fig. 5) is good. For CCl_4, the experimental rate constant is decreasing slightly more rapidly than calculation. Some of the difference can be ascribed to possible experimental error in the slope γ of the underlying cross section, and possibly reflected by the small excursion above the s-wave limit in Fig. 4.

Finally, it is interesting to point out that the calculated $k(\bar{\varepsilon})$ values for both molecules increase, then approach a constant value, as the molecular and electron temperatures approach 0 K. Physically, this corresponds to the distribution $f(\varepsilon)$ narrowing and peaking towards lower energies. At $T < 100$ K $f(\varepsilon)$ samples the portion of $\sigma_A(\varepsilon)$ varying as $\varepsilon^{-1/2}$. And hence the rate constant becomes independent of $\bar{\varepsilon}$ [Eq. (6)]—a direct consequence of the Wigner threshold law for electron attachment near zero electron energy.

ACKNOWLEDGMENTS

The experimental portion of this work was carried out at the Australian National University. We thank A. J. Cullen for implementing the computer control and data acquisition for the CEDS experiment, and S. H. Alajajian for measuring γ for CCl_4 with a new grid structure. Calculations were supported by the U. S. Department of Energy and the National Science Foundation, and were carried out at the Jet Propulsion Laboratory, California Institute of Technology, through agreement with the National Aeronautics and Space Administration.

[1]A. Chutjian, S. H. Alajajian, J. M. Ajello, and O. J. Orient, J. Phys. B **17**, L745 (1984); **18**, 3025(E) (1985).
[2]A. Chutjian and S. H. Alajajian, Phys. Rev. A **31**, 2885 (1985).
[3]R. W. Crompton and G. N. Haddad, Aust. J. Phys. **36**, 15 (1983).
[4]D. Smith, N. G. Adams, and E. Alge, J. Phys. B **17**, 461 (1984).
[5]N. G. Adams, D. Smith, and C. R. Herd, Int. J. Mass Spectrom. Ion Processes **84**, 243 (1988).
[6]D. L. McCorkle, A. A. Christodoulides, L. G. Christophorou, and I. Szamrej, J. Chem. Phys. **72**, 4049 (1980).
[7]A. A. Christodoulides and L. G. Christophorou, J. Chem. Phys. **54**, 4691 (1971).
[8]G. W. Foltz, C. J. Latimer, G. F. Hildebrandt, F. G. Kellert, K. A. Smith, W. P. West, F. B. Dunning, and R. F. Stebbings, J. Chem. Phys. **67**, 1352 (1977).
[9]B. G. Zollars, C. W. Walter, F. Lu, C. B. Johnson, K. A. Smith, and F. B. Dunning, J. Chem. Phys. **84**, 5589 (1986).
[10]B. G. Zollars, K. A. Smith, and F. B. Dunning, J. Chem. Phys. **81**, 3158 (1984).
[11]O. J. Orient and A. Chutjian, in *Abstracts of the Proceedings of the XVth International Conference on Physics of the Electronic and Atomic Collisions, Brighton, 1987*, edited by J. Geddes, H. B. Gilbody, A. E. Kingston, and C. J. Latimer (Queen's University, Belfast, 1987), p. 287.
[12]G. Cavalleri, Phys. Rev. **179**, 186 (1969).
[13]Z. Lj. Petrović and R. W. Crompton, J. Phys. B **17**, 2777 (1985).
[14]O. J. Orient and A. Chutjian, Phys. Rev. A **34**, 1841 (1986).
[15]T. F. O'Malley, Phys. Rev. **150**, 14 (1966).
[16]T. F. O'Malley, Phys. Rev. **155**, 59 (1967).
[17]J. N. Bardsley, Proc. Phys. Soc. London, Sect. B **1**, 349 (1968); J. N. Bardsley, A. Herzenberg, and F. Mandl, in *Atomic Collision Processes*, edited by M. R. C. McDowell (North-Holland, Amsterdam, 1964), p. 415.
[18]E. P. Wigner, Phys. Rev. **73**, 1002 (1948).
[19]S. T. King, J. Chem. Phys. **49**, 1321 (1968) (ω_i for $CFCl_3$).
[20]L. H. Jones, B. I. Swanson, and S. A. Ekberg, J. Phys. Chem. **88**, 5560 (1984) (ω_i for CCl_4).
[21]M. W. Long, Q. Williams, and T. L. Weatherly, J. Chem. Phys. **33**, 508 (1960) (B_v for $CFCl_3$).
[22]S. Yamamoto, M. Takami, and K. Kuchitsu, J. Chem. Phys. **81**, 3800 (1984) (B_v for CCl_4).
[23]A. Chutjian, J. Phys. Chem. **86**, 3518 (1982).
[24]S. H. Alajajian, M. T. Bernius, and A. Chutjian, J. Phys. B **21**, 4021 (1988).
[25]The neutral-molecule curves $V_i(R)$ are of the Lennard-Jones form, with $D_e = 3.05$ eV and $R_e = 1.760$ Å for CCl_4; and 3.08 eV, 1.766 Å for CCl_4.